Volume 14, Number 3, 2021. pp. 221-230

Jordan Journal of Physics

ARTICLE

Investigating the Effect of Nitro Groups on the Electronic Properties of Phenanthrene Compound

Haider O. Essa[a] and **Satha M. Abbas**[b]

[a] *Biology Department, Science College, Al-Qasim Green University, Al-Qasim Town, Babylon Province, 51013, Iraq.*

[b] *Chemistry and Physiology Department, Veterinary Medicine College, Al-Qasim Green University, Al-Qasim Town, Babylon Province, 51013, Iraq.*

Doi: **https://doi.org/10.47011/14.3.4**

Received on: 13/05/2020; Accepted on: 13/9/2020

Abstract: Theoretical study for calculating the electronic structure of phenanthrene compound and its simplest derivatives with nitro groups in different positions was performed using density functional theory (DFT) based on the hybrid function of three parameters. Lee-Yang-Parr [B3LYP] with 6-31 [d, p] basis set was used to investigate the effect of nitro groups on the electronic properties of phenanthrene compound. All calculations were obtaind by employing the used method using the Gaussian 09 package of programs. The energy gaps, total energies, the energy of HOMO and LUMO, softness, dipole moment, Fermi level, molecular symmetry, electrochemical hardness, electron density, electrostatic potential surfaces and infrared spectra were calculated. The results showed that the electronic properties of phenanthrene molecule are affected by the added nitro group. The total energy, energy gap and the HOMO and LUMO energy decreased compared with the original molecule. The ionization potential (IP), electron affinity (EA) and Fermi level (Ef) are increased compared with the original molecule.

Keywords: B3LYP/DFT calculations, Phenanthrene molecule, Nitro group, Energy gap, Ionization potential.

Introduction

Polycyclic aromatic hydrocarbons (PAHs) are a large group of organic compounds with two or more combined aromatic rings. PAHs are mainly generated as a result of pyrolysis processes, especially incomplete combustion of organic matter during industrial and other human activities, such as coal and crude oil processing, natural gas combustion including for heating, waste combustion, vehicle movement, cooking and smoking, as well as in natural processes, such as carbonation [1, 2]. Cytotoxicity is one of several important biological effects of polycyclic aromatic hydrocarbons. Therefore, many intensive efforts have been made for the discovery and development of new cytotoxic molecules [3, 4]. The PAH phenanthrene was studied in this paper. Phenanthrene is the simplest non-linear polycyclic aromatic hydrocarbon with three benzene ring structure. It is a colorless crystal with luster and phenanthrene precipitated from ethanol is a colorless monoclinic crystal. It is a leaf-like crystal with a relative density of 1.179 (25/4 °C), a refractive index of 1.6450, a melting point of 101 °C and a boiling point of 340 °C. Though it can sublime, it is insoluble in water, slightly soluble in ethanol, soluble in ether, benzene, acetic acid, chloroform, carbon tetrachloride and carbon disulfide [5, 6]. Phenanthrene can be used in the manufacture of pesticides and dyes and can also be used in stabilizing high-efficiency and low-toxicity pesticides, as well as smokeless powder explosives [7]. Phenanthrene has an anti-cancer property against human colonnade

Corresponding Author: Haider O. Essa **Email**: headeromran@yahoo.com

epithelial cancer cell lines [8]. Due to the chemical and physical properties of the phenanthrene molecule, there are many studies on its electronic structure, where Ayşegül Gümüş *et al.* studied computationally a series of phenanthrene and phenanthroline derivatives to investigate their potential usage as organic solar cell components, thermally activated delayed fluorescence and nonlinear optic compounds [9]. Alan Hinchliffe *et al.* studied molecular polarizabilities for anthracene and phenanthrene [10] and P.L. de Andres *et al.* studied the electronic and geometrical structure of potassium-doped phenanthrene [11]. In the present work, we chose the effect of nitro groups, because nitro groups are organic compounds that contain one or more nitro functional groups ($-NO_2$) and are also strongly electron-withdrawing. Because of this property, C−H alpha bonds to the nitro group can be acidic [12]. Two nitro groups were used in the present work to achieve substitution patterns (Iso, Para, Meta). The main aim of this paper is to determine the effect of nitro groups on the electronic properties of phenanthrene compound by using density functional theory with 6-31G (d, p) basis set.

Theoretical Model

The electronic structure of organic compounds is essential to the realization of virtually all the properties of materials, including the arrangement of atoms and molecules, electronic properties, mechanical properties and thermodynamic properties [13]. Density functional theory (DFT) is a quantum mechanical method which can be applied to study the electronic structure for organic compounds. For the past 30 years, density functional theory has been the predominant method for the quantum mechanical simulation of periodic systems. In recent years, it has also been adopted by quantum chemists and is now widely applied for the simulation of energy surfaces in molecules [14, 15]. The electronic structure of phenanthrene compound has been studied by density functional theory (DFT).Three parameters B3LYP (Becke's three parameter exchange with Lee, Yang and Parr correlation functional) density functional theory with 6-31G (d, p) basis set [16-19] are used in this paper to perform the ground state calculations. Full geometry optimizations of phenanthrene molecule were drawn on Gauss View 5.0.8 [20] and relax using the Gaussian 09 package of programs [21], as shown in Fig. 1. The hybrid exchange-correlation functional B3LYP is very effective for computing the electronic properties of phenanthrene molecule, such as total energy, energy of HOMO and LUMO, energy gap, ionization potential (IP), electron affinity (EA), hardness (H) and softness (S) [22-24]. The total energy (E_T) clarifies the sum of potential energy and kinetic energy of the system [25, 26]. HOMO refers to the highest occupied molecular orbitals and LUMO symbolizes the lowest unoccupied molecular orbitals. The energy gap is the variation of the energies between the HOMO and LUMO levels [25, 27]. The ionization potential (IP) for a molecule is the magnitude of energy needed to separate an electron from an isolated atom or molecule; HOMO energy was also applied to calculate IP in the framework of Koopman's theorem $IP = - E_{HOMO}$ [28-30]. The LUMO energy was also applied to compute the electron affinity (EA) of a molecule according to Koopman's theorem $EA = - E_{LUMO}$ [28, 30, 31]. One of the global quantities is chemical potential (μ); it measures the escaping tendency of an electronic cloud and is defined by $\mu = (E_{HOMO} + E_{LUMO}) / 2$ [31]. The hardness (H) is a measurement of molecule resistance to the change or deformation and is defined by $H = (IP-EA)/2$ [31]. The global chemical softness (S) is a property of molecules that measures the extent of chemical reactivity. It is the inverse of hardness and is given as: $S = 1/2H$ [32, 33]:

Results and Discussion

In this section, we present the results of our work and discuss the electronic properties of phenanthrene molecule. Table 1 displays the energy gaps, electronic states such as the lowest unoccupied molecular orbital (LUMO) and the highest occupied molecular orbital (HOMO), total energies and the symmetry of structures for molecules studied.

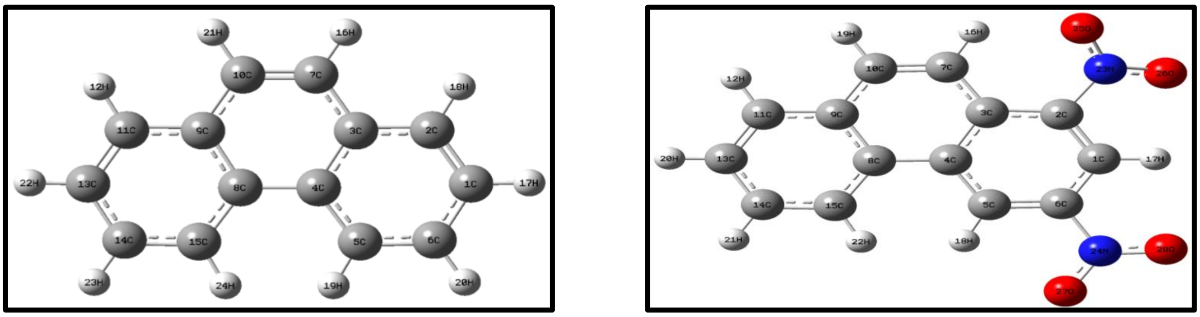

1 (Phenanthrene) **2 (2, 6 – dinitrophenanthrene)**

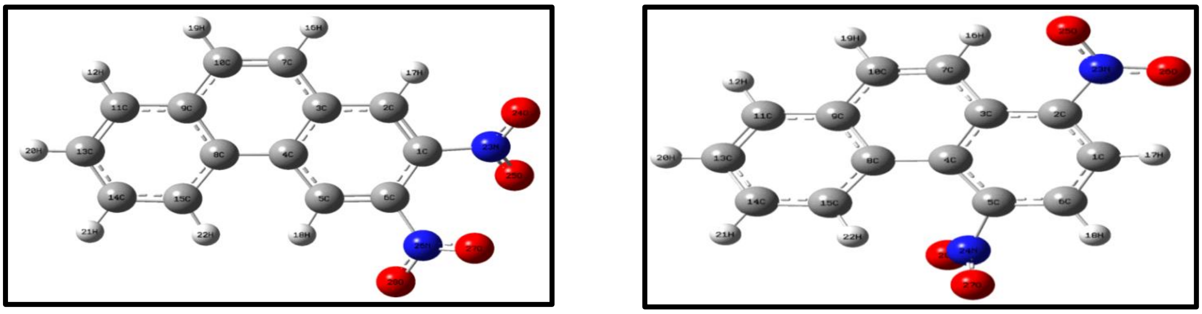

3 (1, 6 – dinitrophenanthrene) **4 (2, 5 – dinitrophenanthrene)**

FIG. 1. The optimized structures of phenanthrene molecule and its derivatives with nitro groups in different positions.

TABLE 1. Total energy, symmetry, HOMO – LUMO and energy gap for molecules.

Mol.	Total energy (a.u.)	Symmetry	HOMO (eV)	LUMO (eV)	HOMO (eV) [9]	LUMO (eV) [9]	Energy gap (eV)	Energy gap (eV) [9]
1	-539.419	C_1	-5.77118	-0.99239	–5.75	–1.01	4.778796	4.74
2	-948.247	C_1	-6.91867	-3.48382	-----	----	3.434845	----
3	-948.235	C_1	-6.90397	-3.35729	-----	------	3.546682	----
4	-948.227	C_1	-6.73799	-3.56845	-----	-----	3.169537	----

From Table 1, the electronic properties of phenanthrene molecule are affected by the addition of nitro groups, where the total energy, energy gap and the HOMO and LUMO energy decreased compared with the original molecule, as shown in Figs. (2-4), respectively. Decreasing the energy gap improves the conductivities and increases the solubility of these molecules. Also, it is clear from Table 1 that the total energy, energy gap and the HOMO and LUMO energy for all dinitrophenanthrene molecules are approximately pointing to the fact that the electronic properties are independent on the position of the nitro radical in the ring. The symmetry of the studied molecules is C1, meaning that the studied molecules have only one symmetry operation. Fig. (5) illustrates the 3-D distribution of HOMOs and LUMOs for the studied molecules.

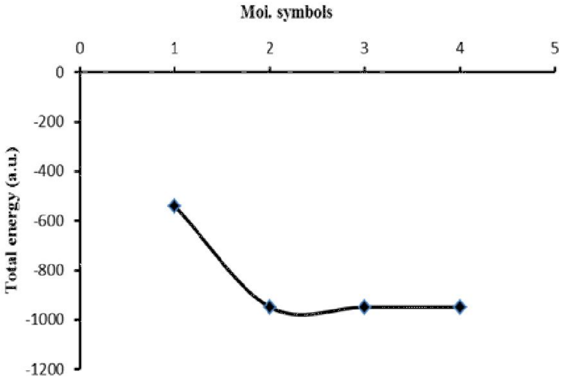

FIG. 2. The calculated total energy for molecules under study.

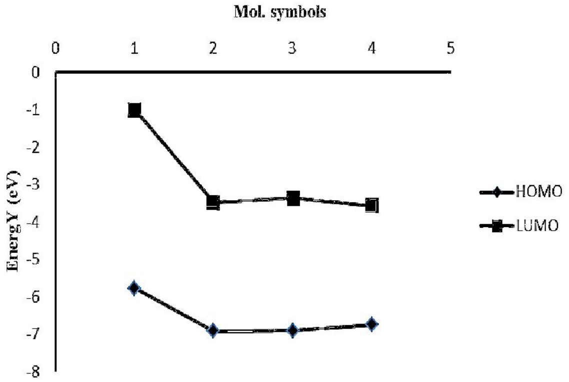

FIG. 3. The HOMO and LUMO energies for molecules under study.

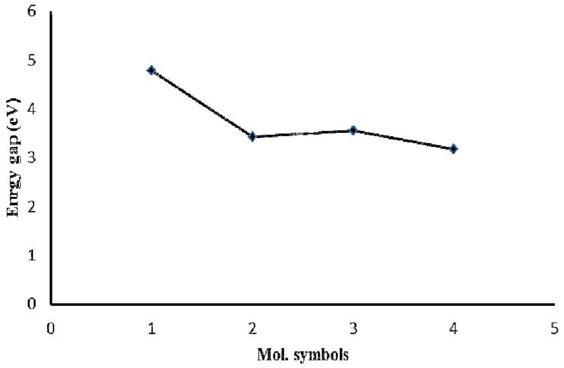

FIG. 4. The calculated energy gaps for molecules under study.

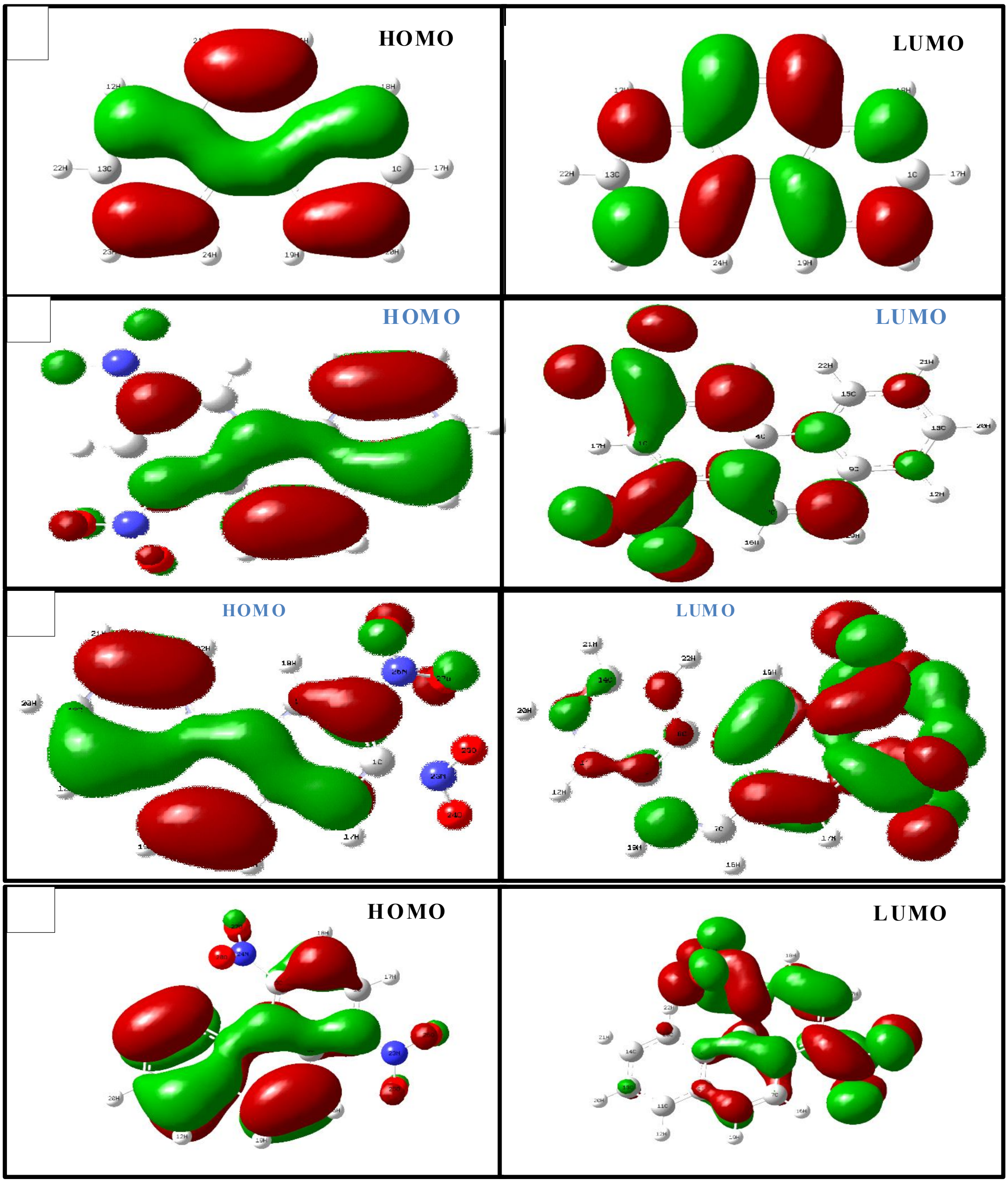

FIG. 5. HOMO and LUMO shapes of the phenanthrene and dinitrophenanthrene molecules.

Fig. 5 shows the electronic density distribution along the rings C-C. In the different parts of dinitrobiphenyl molecules, the electronic density distribution is homogeneous. It was noticed for all molecules that HOMO shows a bonding character and LUMO shows an antibonding character.

From Table 2, the ionization potential (IP), electron affinity (EA) and Fermi level (Ef) are affected by the addition of nitro groups, where they are increased compared with the original molecule, as shown in Figs. (6, 7), respectively. The ionization potential (IP), electron affinity (EA) and Fermi level (Ef) for all dinitrophenanthrene molecules are approximately the same, indicating that the electronic properties are independent on the position of the nitro radical in the ring. The softness (S) and hardness (H) values for all dinitrophenanthrene molecules are slightly lower comparable to original molecule, as shown in Fig. 8; this is because nearly all the usually used exchange-correlation functionals such as B3LYP, B3PW91 and Koopman's theorem, satisfy accuracy. Adding nitro groups leads to change the values of the dipole moment (μ), where the phenanthrene molecule has no dipole moment and is planar in space. Adding the subgroups leads to varying the symmetrical distribution of the electronic structure of the molecule, therefore changing the dipole moment, as shown in Fig. 9.

TABLE 2. The electronic properties of studied molecules.

Mol.	IP (eV)	EA(eV)	Ef (eV)	H (eV)	S (eV)	μ
1	5.771181	0.992385	6.267374	5.274988	2.637494	0.0341
2	6.918669	3.483824	8.660581	5.176757	2.588378	7.5606
3	6.903975	3.357293	8.582622	5.225328	2.612664	9.9884
4	6.737988	3.568451	8.522213	4.953763	2.476881	3.2225

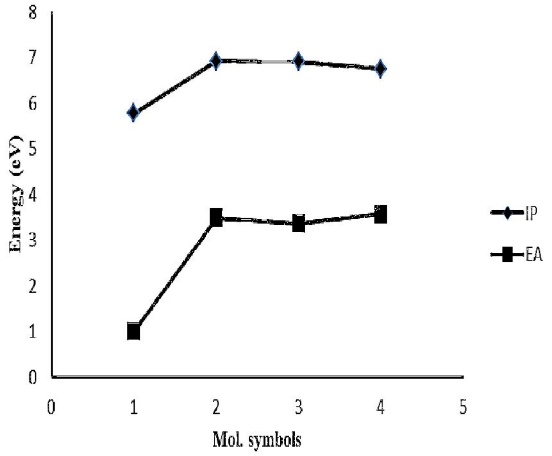

FIG. 6. The calculated ionization potential (IP) and electron affinity (EA) for molecules under study.

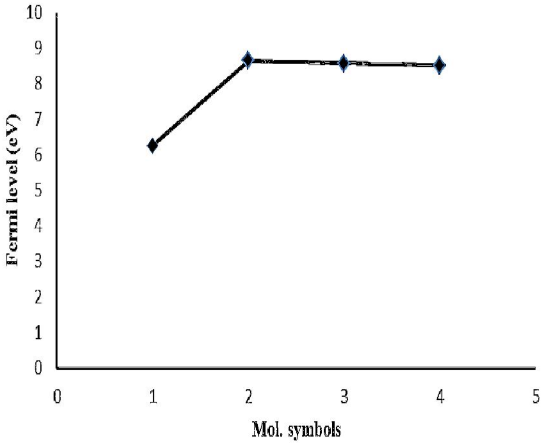

FIG. 7. The calculated Fermi level for molecules under study.

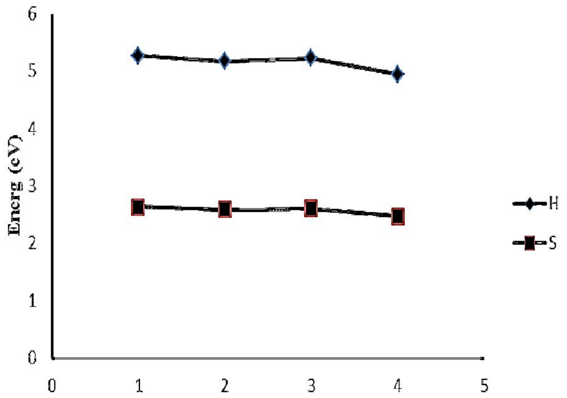

FIG. 8. The calculated hardness (H) and softness (S) for molecules under study.

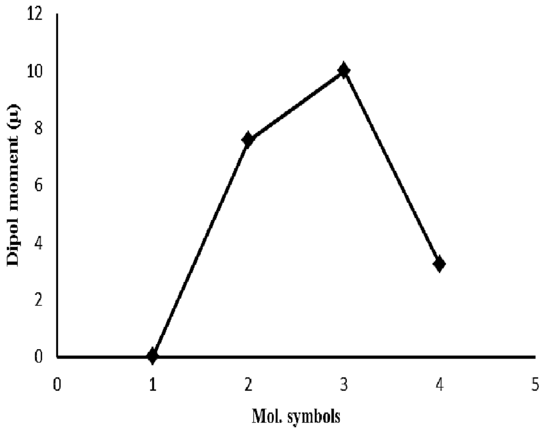

FIG. 9. The calculated dipol moment for molecules under study.

Electron Density Surface

Fig. 10 explains the three-dimensional shape of electron density distribution surface of phenanthrene and dinitrophenanthrene molecules, where the electron density was distributed due to the distribution of all atoms in the space of the complex according to the total density of the electrons in the complex. The total density is useful for understanding bonding and reactivity [34]. From this figure, it can be seen that the electron density distribution surface for the studied molecules is asymmetric, where the electron density is dragged towards the atoms of high electronegativity.

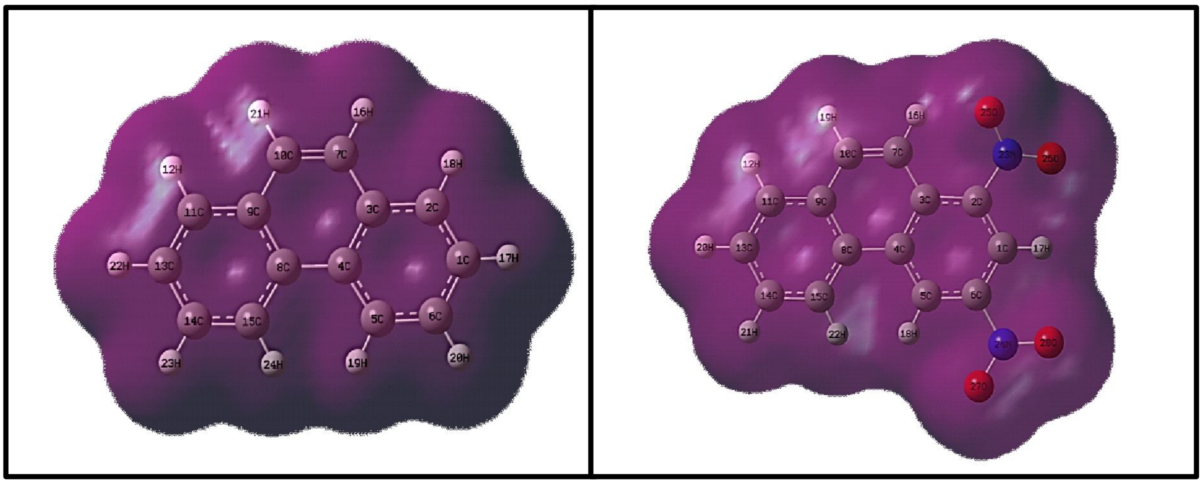

1 (Phenanthrene)

2 (2, 6 – dinitrophenanthrene)

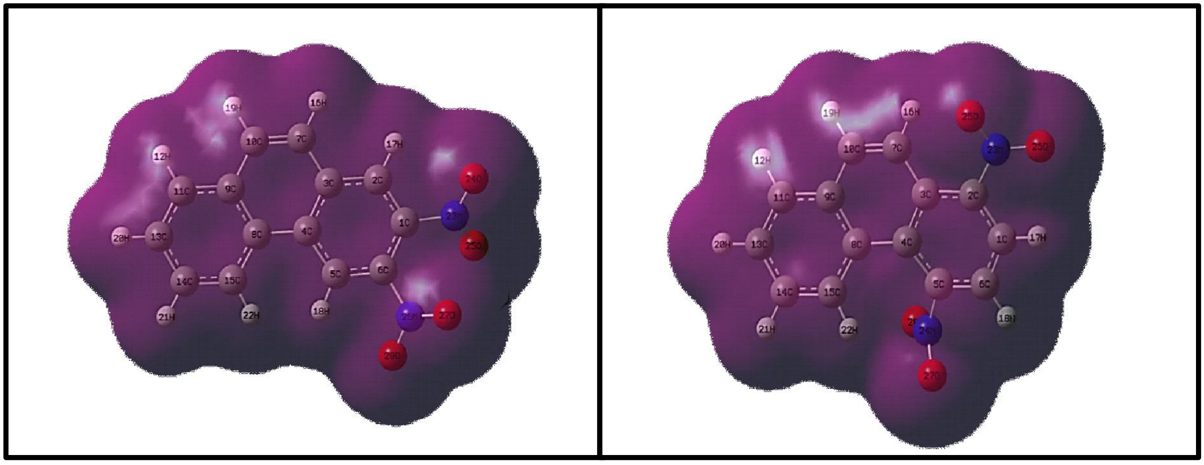

3 (1, 6 – dinitrophenanthrene)

4 (2, 5 – dinitrophenanthrene)

FIG. 10. The electron density distribution for molecules under study.

Electrostatic Potential Surface

Fig. 11 explains the distribution of electrostatic potential, which depends on the negative and positive charges and depends also on the electronegativity of the atoms in the phenanthrene and dinitrophenanthrene molecules. In general, the electrostatic potential surfaces are dragged towards the atoms of high electronegativity.

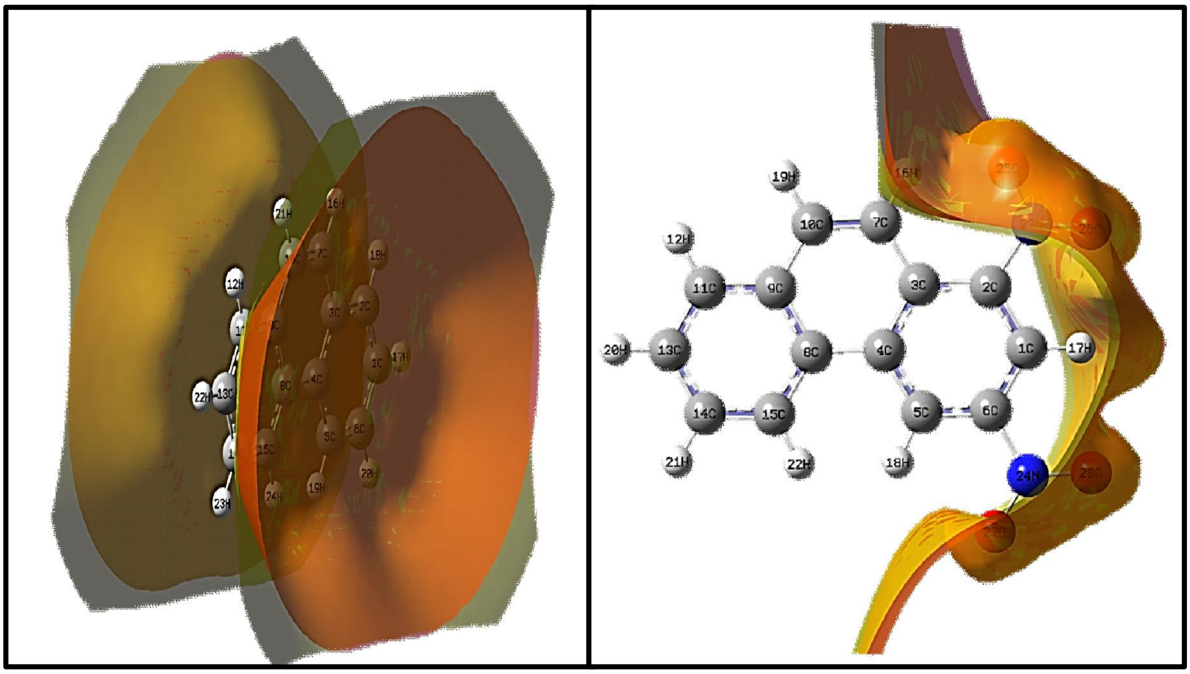

1 (Phenanthrene) **2 (2, 6 – dinitrophenanthrene)**

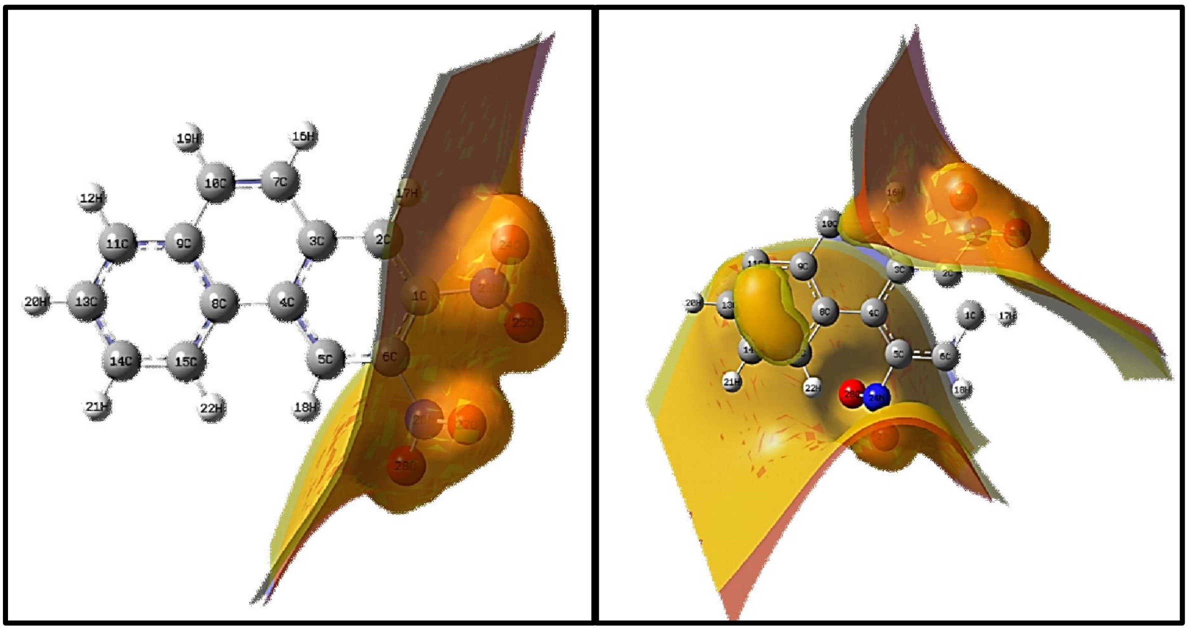

3 (1, 6 – dinitrophenanthrene) **4 (2, 5 – dinitrophenanthrene)**

FIG. 11. The electrostatic potential surfaces for molecules under study.

Infrared Spectra

Fig. 12 shows the computed IR spectra for phenanthrene and dinitrophenanthrene molecules. The harmonic vibrational frequencies were calculated for the studied molecules by using B3LYP level with a 6-31G basis set. The substitution of hydrogen atoms by NO_2 leads to increasing the number of vibrational modes. According to the rule of (3N-6), the phenanthrene molecules have 66 degrees of freedom, while the dinitrophenanthrene molecules have 78 degrees of freedom. All degrees of freedom for phenanthrene **1** and its derivatives **2-4** are represented by stretching, bending, rocking and scissoring modes. The (C – H) stretching vibrations of aromatic molecules are characteristic in the region (2900–3250) cm^{-1} which is a characteristic region for ready identification of (C – H) stretching vibrations and particularly the region (3250–3100) cm^{-1} for asymmetric stretching and (3100–2900) cm^{-1} for symmetric stretching modes of vibration [35]. For a phenanthrene molecule, the (C–H) stretching has been studied around 3197.81 cm^{-1}. The (C-C) stretching vibrations have been studied in the region 1681.13 cm^{-1}. Also, Figure (12) shows the IR spectrum of dinitrophenanthrene molecules **2-4** which has new peaks in the vibration modes in comparison with phenanthrene molecule **1,** due to the existence of stretched bonds, such as (C-N), (C-H) and (N-O) for **2-4** molecules. The stretching of (C-H) has been observed in the range of 3285.46-3293.51 cm^{-1}. The (C-N) stretching has been observed in the region 1656.08-1134.30 cm^{-1}, whilst the stretching of (C-C) bond is shown in the range of 1675.12-1661.38 cm^{-1} and the stretching of (N-O) bond is shown in the region 1493.81-1352.20 cm^{-1}.

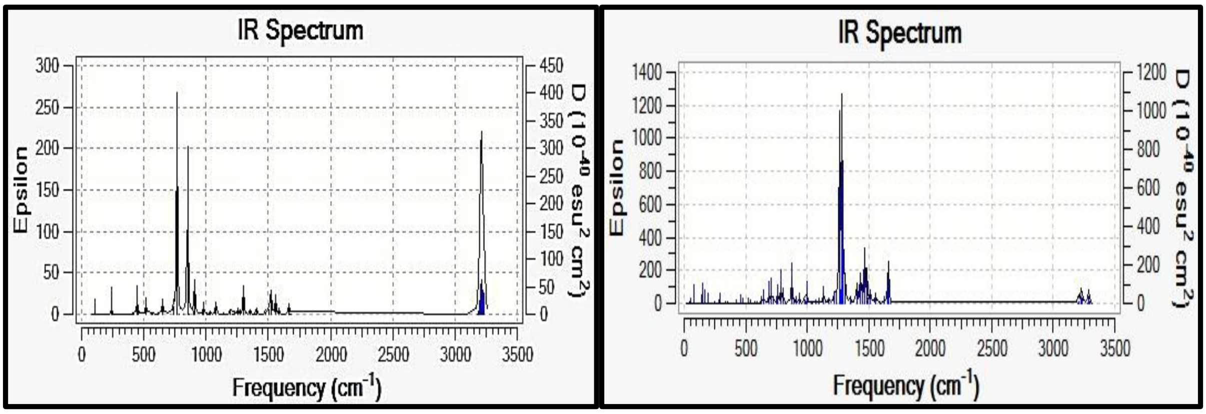

1 (Phenanthrene) **2 (2, 6 – dinitrophenanthrene)**

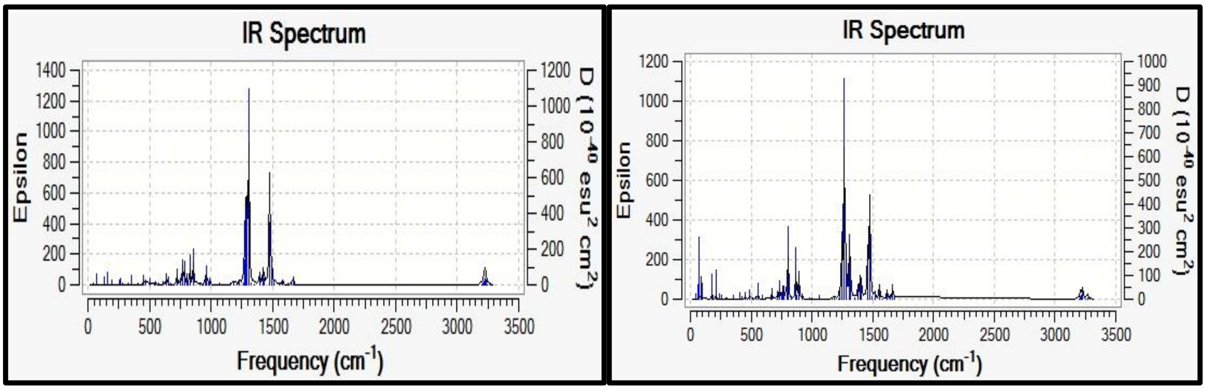

3 (1, 6 – dinitrophenanthrene) **4 (2, 5 – dinitrophenanthrene)**

FIG. 12. The calculated IR spectral frequencies for molecules under study.

Conclusions

Density functional [B3LYP/6-31 G(d, p)] theoretical methodology has been concerned with the determination of geometrical and energetic features in order to identify the factors influencing the values of ionization potential and electron affinity computed by orbital vertical theory (Koopman's theorem). Also, electronic properties, such as total energy, HOMO and LUMO energies, energy gap, chemical hardness, softness, dipole moment, electron density surface, electrostatic potential surface and spectroscopic properties such as IR spectra were investigated for the phenanthrene and dinitrophenanthrene molecules. The addition of nitro groups affected the electronic structure of phenanthrene molecule, where the total energy energy gap and the HOMO and LUMO energy, decreased compared to the original molecule and the ionization potential (IP), electron affinity (EA) and Fermi level (Ef) show an increase compared with the original molecule. The electronic properties are independent on the position of the nitro radical in the ring. Electron density and electrostatic potential surfaces are dragged towards atoms of high electronegativity. The substitution of hydrogen atoms by NO_2 led to an increase in the number of vibrational modes.

References

[1] Danzon, M.A., “Air Quality Guidelines”, 2nd edition, (WHO Regional Office for Europe, Copenhagen, Denmark, 2000).

[2] Lerda, D., “Polycyclic aromatic hydrocarbons (PAHs) factsheet”, 4th edition, (European Union, 2011).

[3] Zhang, H.Z., Kasibhatla, S., Kuemmerle, J., Kemnitzer, W., OllisMason, K., Qiu, L., Crogan-Grundy, C., Tseng, B., Drewe, J. and Cai, S.X., J. Med. Chem., 48 (2005) 5215.

[4] Mattson, M.P., Brain Pathol., 10 (2000) 300.

[5] Singh, L., Varshney, J.G. and Agarwal, T., Food Chemistry, 199 (2016) 768.

[6] de Azeredo, S.O.F. and Figueroa-Villar, J.D., World Journal of Pharmacy and Pharmaceutical Sciences, 3 (11) (2014).

[7] Samimi, S.V., Akbari Rad, R. and Ghanizadeh, F., Iran J. Environ. Health Sci. Eng., 6 (1) (2009) 47.

[8] Guedouar, H., Aloui, F., Beltifa, A., Ben Mansour, H. and Ben Hassine, B., C. R. Chimie, 20 (2017) 841.

[9] Gümüş, A. and Gümüş, S., Macedonian Journal of Chemistry and Chemical Engineering, 36 (2) (2017) 239.

[10] Hinchliffe, A. and Soscun Machado, H.J., Int. J. Mol. Sci., 1 (2000) 8.

[11] de Andres, P.L., Guijarro, A. and Verges, J.A., “Instituto de Ciencia de Materiales de Madrid (CSIC)”, (28049 Madrid, Spain, 2018).

[12] Ju, K.-S. and Parales, R.E., Microbiol. Mol. Biol. Rev., 74 (2) (2010) 250.

[13] Irene, E.A., “Electronic Materials Science”, (John Wiley & Sons, Inc., Hoboken, New Jersey, 2005).

[14] Fitts, D.D., “Principles of Quantum Mechanics As Applied to Chemistry and Chemical Physics”, (Cambridge University Press, New York, 2002).

[15] Rogers, D.W., “Computational Chemistry Using the PC”, 3d Edition, (John Wiley & Sons, Inc., Hoboken, New Jersey, 2003).

[16] Reimers, R.J., “Computational Methods for Large Systems: Electronic Structure Approaches for Biotechnology and Nanotechnology”, (John Wiley & Sons, Inc., Hoboken, New Jersey, 2011).

[17] Jones, R.O., Reviews of Modern Physics, 87 (2015) 897.

[18] Sahni, V., “Quantal Density Functional Theory II: Approximation Methods and Applications”, (Springer Verilog, Berlin, Heidelberg, 2010).

[19] Stephens, P.J., Devlin, F.J., Chabalowski, C.F. and Frisch, M.J., The Journal of Physical Chemistry, 98 (43) (1994) 11624.

[20] Roy, D.D., Todd, A.K. and John, M.M., “Gauss View 5.0.8. Gaussian”, (Gaussian, Inc., Wallingford, 2009).

[21] Frisch, M.J., Trucks, G.W., Schlegel, H.B. et al., “Gaussian 09, Revision A.02", (Gaussian, Inc., PA, Wallingford CT, 2009).

[22] Engelberts, J., Havenith, R., Van Lenthe, J., Jenneskens, L. and Fowler, P., Inorg. Chem., 44 (2005) 52266.

[23] Santos, J.C.J., Andres, A., Aizman, P. and Fuentealba, J., Chem. Theory Comput., 1 (2005) 83.

[24] Santos, J.C., Tiznado, W., Contreras, R. and Fuentealba, P., J. Chem. Phys., 120 (2004) 1670.

[25] Nagarajan, V. and Chandiramouli, R., International Journal of Chem. Tech. Research, 6 (1) (2014) 21.

[26] Zarkadoula, E.N., Sharma, S., Dewhurst, J.K., Gross, E.K.U. and Lathiotakis, N.N., Physical Review A, 85 (2012) 1.

[27] Zhuo, L.G., Liao, W. and Yu, Z.X., Asian Journal of Organic Chemistry, 1 (2012) 336.

[28] Zhan, C., Nichols, J.A. and Dixon, D.A., Journal of Physics and Chemistry A, 107 (2003) 4184.

[29] Karzazi, Y., Belghiti1, M.E., El-Hajjaji, F. and Hammouti, B., Journal Mater. Environ. Sci., 7 (10) (2016) 3916.

[30] Hinchliffe, A., “Molecular Modelling”, (John Wiley & Sons, Ltd., England, 2003).

[31] Mueller, M., “Fundamentals of Quantum Chemistry: Molecular Spectroscopy and Modern Electronic Structure Computations”, (Kluwer Academic/ Plenum Publishers, New York, 2001).

[32] Abel Kolawole, O. and Banjo, S., Analytical & Bioanalytical Electrochemistry, 10 (1) (2018) 136.

[33] Reyes, R.V. and Aria, A., Journal Ecl. Quim., Sao Paulo, 33 (3) (2008) 69.

[34] Cramer, C.J., “Essentials of Computational Chemistry”, (John Wiley & Sons, Ltd., USA, 2004).

[35] Sadasivam, K. and Kumaresan, R., Computational and Theoretical Chemistry, 963 (2011) 227.